JOURNAL OF MATERIALS SCIENCE 8 (1973) 1527–1533

Crack propagation studies in brittle materials

S. W. FREIMAN, D. R. MULVILLE, P. W. MAST
Naval Research Laboratory, Washington DC, USA

An analysis was made of cantilever beam specimens used for crack propagation studies. Included in this analysis were the effects of a plastic zone at the crack tip, beam rotation, and the viscoelastic response of the material. This analysis showed that application of a constant bending moment to the specimen rather than a constant load provides a test in which the strain energy release rate, $\mathscr{G}$, is independent of crack length. Other advantages of this test configuration are that corrections for shear or beam rotation effects are not necessary. Results of this test on both glass and ceramics are reported.

List of symbols

a = crack length
A = cross-sectional area of beam
b = total thickness of specimen
d = deflection of loading arm
E = elastic modulus of material
E_1 = dynamic modulus
E_2 = transient response modulus
G = shear modulus of material
$\mathscr{G}$ = strain energy release rate
$\mathscr{G}_{vE}$ = strain energy release rate of viscoelastic material
h = half height of specimen
I = moment of inertia of cantilever beam = $bh^3/12$
k = modulus of elastic foundation
K = stress intensity factor
L = distance from point of load application to fulcrum of loading arm
L' = distance from point at which arm deflection is measured to fulcrum
M = applied bending moment
P = force applied to beam
r = length of plastic zone
t = thickness of specimen at groove
T = force applied to loading arm
u = displacement of beam
V = crack velocity
w = half height of groove
W = stored elastic energy
δ = characteristic length of beam on elastic foundation
λ = reciprocal of the characteristic length of beam
θ = rotation of beam
X = viscoelastic creep compliance function
ψ = time
$\triangle$ = inherent opening distance as defined by Wnuk [10]
σ_y = yield strength of material
ν = Poisson's ratio

1. Introduction

The strength of brittle materials is determined to a great extent by their resistance to crack propagation. The fracture strength is a function of a number of parameters including elastic modulus, flaw size and "fracture energy". The latter term is normally used to indicate the strain energy release rate, $\mathscr{G}$, needed to initiate fast fracture. Ceramics can fail, however, under stresses much less than which will cause immediate fracture, but which in combination with the environment can cause slow crack growth from existing surface flaws. Knowledge of both crack velocity and acceleration under a given loading can enable one to predict the lifetime of the material under stress.

The tests most widely used in studies of stable crack propagation have been the double cantilever [1-3] and the double torsion [4, 5] although other configurations have been employed. Evans [6] has recently shown that application of constant deflection to a double torsion specimen can be an efficient method of obtaining crack propagation data. The double cantilever test is the most commonly used. Because of the great sensitivity of ceramics to

changes in strain energy release rate, $\mathcal{G}$, a major disadvantage of this test is the fact that $\mathcal{G}$ is dependent on crack length. Use of a correctly tapered sample [7] can solve this problem but the machining of these specimens is difficult. In the double torsion test, there is no dependence of $\mathcal{G}$ on crack length but the test has the disadvantage that the crack shape is not geometrically simple.

Contained in this paper is a general analysis employing beam theory and beam on an elastic foundation theory of cantilever beam specimens including the effects on $\mathcal{G}$ of a plastic zone at the crack tip, beam rotation ahead of the crack and a viscoelastic response of the material. An outgrowth of this analysis is the conclusion that an especially efficient test configuration is one in which a constant bending moment is applied to a double cantilever beam. Results of this test on glass and ceramics are presented.

2. Theory

The analysis of the double cantilever beam is based on the specimen configuration shown in Fig. 1. The purpose of the groove down the centre of the specimen is to guide the crack. Its depth and width is designed to prevent the flow or fracture stress in the specimen arms from becoming critical.

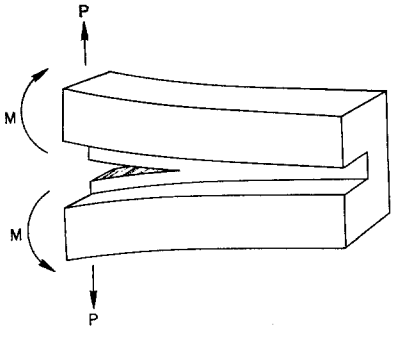

Figure 1 Schematic of double cantilever beam specimen.

For the purpose of analysis, this specimen is assumed to be equivalent to that of a semi-infinite beam on an elastic foundation as shown in Fig. 2. This beam can be analysed in three parts: the cantilever part ($x = 0$ to a), the ideal plastic zone ($x = a$ to $a + r$) and the portion analysed as a beam on elastic foundation ($x > a + r$). When the crack extends or the plastic

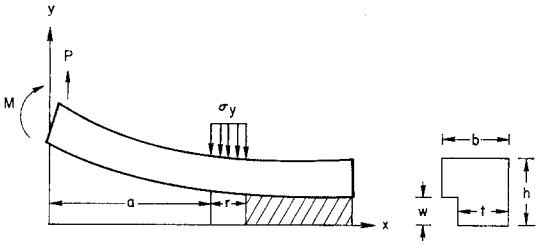

Figure 2 Detailed schematic of cantilever beam as analysed in this study.

zone grows, the change in the stored elastic energy in the specimen can be obtained as a sum of the energy changes in the three parts. The details of this analysis are given in the Appendix.

These results can be summarized as follows*.

1. Cantilever beam

$$\frac{dW}{da} = \frac{1}{2EI}\left[(M + Pa)^2 + \frac{EIP^2}{GA}\right] \tag{1}$$

2. Plastic zone

$$\frac{dW}{dr} = \frac{1}{2EI}\left[\left(M + P(a + r) - \frac{\sigma_y r^2}{2}\right)^2 + \frac{EI}{GA}(P - \sigma_y r)^2\right] \tag{2}$$

3. Beam on elastic foundation

$$dW = \frac{\partial W}{\partial a}da + \frac{\partial W}{\partial r}dr$$

where

$$W = \frac{\delta}{2EI}\left(\frac{\delta^2 P'^2}{2} + \delta P' M'' + M''^2\right)$$

and

$$P' = P - \sigma_y r \tag{3}$$

$$M' = M + P(a + r) - \frac{\sigma_y r^2}{2}\cdot$$

The general expression for the change in stored elastic energy is obtained by adding the results of the three parts, i.e. Equations 1, 2 and 3.

As an example of the usefulness of this analysis, consider the usual double cantilever test on a brittle material in which $M = 0$ and $dr = 0$. In this case Equation 2 also equals zero and Equations 1 and 3 reduce to

$$\frac{dW}{da} = \frac{P^2}{2EI}\left(a^2 + \frac{EI}{GA} + \delta^2 + 2a\delta\right)\cdot \tag{4}$$

*The change in stored energy with change in crack length represents the energy change due to both bending and shear.

The right hand side of Equation 4 contains a perfect square in $a + \delta$ and can be written as

$$\frac{dW}{da} = \frac{P^2}{2EI}\left[(a + \delta)^2 + \frac{EI}{GA}\right]. \quad (5)$$

The contribution owing to shear is EI/GA, while the contribution owing to rotation is a crack which appears longer than actually viewed, by the amount δ*. Taking t as the thickness of the beam at the crack tip the strain energy release rate for this configuration is given by

$$\mathcal{G} = \left(\frac{2}{t}\right)\frac{dW}{da} = \frac{P^2a^2}{EIt}\left[\left(1 + \frac{\delta}{a}\right)^2 + \frac{E}{12G}\left(\frac{h}{a}\right)^2\right]. \quad (6)$$

Equation 6 is similar to expressions for $\mathcal{G}$ discussed by Gillis and Gilman [2] and Wiederhorn *et al* [3].

Using the fact that $E = 4G(1 + \nu)$ for a beam, the coefficient of the shear term for $\nu = 0.2$ becomes $(1 + \nu)/3 = 0.40$ compared to a commonly used value of 0.45 in [3].

If, however, only a moment, M, is applied to the double cantilever specimen (P and $dr = 0$), it follows from Equations 1 to 3 that a test can be devised which yields a much simpler expression for $\mathcal{G}$.

$$\frac{dW}{da} = \frac{M^2}{2EI} \quad (7)$$

$$\mathcal{G} = \frac{M^2}{EIt}. \quad (8)$$

The significant aspects of this test are that $\mathcal{G}$ is independent of crack length and plastic zone size (provided $dr = 0$). It is also seen that for this arrangement no contributions to $\mathcal{G}$ exist owing to either shear or beam rotations ahead of the crack. There are end effects, however, owing to the fact that the specimen is not a semi-infinite beam. When the crack reaches a distance approximately equal to δ from the end of the specimen the test become invalid. Another advantage of this technique is its adaptability for the analysis of viscoelastic behaviour described in the Appendix.

3. Experimental technique

A shown in Fig. 3, a constant moment (TL) is achieved by applying a constant load to the ends of arms attached to the top of a double cantilever beam specimen. In most cases these arms are machined from metal so that the sample can be inserted into them and clamped into place. Where clamping is undesirable, arms can be affixed to the specimen with epoxy cement. Inserts in the arms keep the sample parallel to the loading plane during testing. By preparing a number of inserts for the arms, samples of different thicknesses can be tested. The inserts are clamped against the sample by means of a pointed screw extending through each arm. The arms are machined so that they can consistently be placed in the same position in the loading fixture.

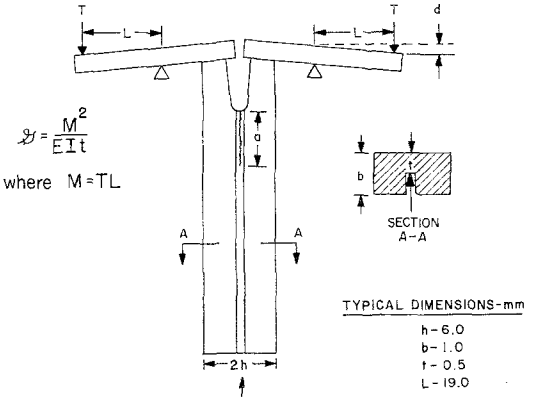

Figure 3 Specimen configuration employed in constant moment type test; loading arms are shown affixed to the top of the specimen.

Fig 4 shows the arrangement of the sample in the loading fixture. The top portion of the fixture is hinged to allow the arms to open as the crack propagates. The triangular portion at the bottom assures that the load is divided equally between the two sides. The movable head is connected to the sample arms through wires attached to sleeves which slip over the arms. Springs placed in the load train reduce disturbances to the system. The sample is loaded through ball bearings in the sleeves which rest in dimples in the top of the arms.

While dead weight loading can be used, a greater flexibility in test procedure may be achieved through the use of a closed loop loading system. In this case, the output voltage

*This effect was first observed in adhesive joints by Charles Fowlkes of the Naval Research Laboratory in 1960.

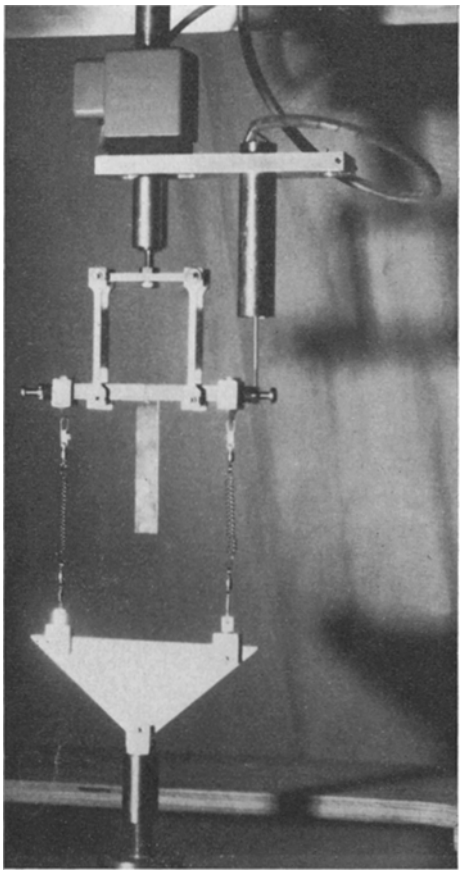

Figure 4 Specimen arrangement in loading fixture. The fixture is in the closed loop test system. DCDT is to right of loading fixture.

from the load cell is amplified and fed into an electrohydraulic servo controller of ram displacement*. By dialing in a given command voltage on a potentiometer, the desired load can be produced. The output of the load cell is also fed, after amplification and scaling into a digital voltmeter which allows the experimenter to directly observe the load on the sample.

Crack velocities can be determined in two ways, either by visual observation in a travelling microscope or by measurement of the compliance change in the arms as the crack propagates. In the latter case, the deflection, d, of an arm as shown in Fig. 3, is measured using a DCDT†, whose output voltage has been amplified and fed into a chart recorder. For most materials, deflection is measured in micro-inches, making it necessary to amplify the output from the DCDT by 100 in order to see small changes in d. Crack velocity can then be determined from the plot of d versus time through Equation 9, which is obtained from the geometry and compliance of the system.

$$a = \frac{EI}{ML'} d \tag{9}$$

4. Test procedure and results

Since the primary purpose of this paper is to describe a test procedure, only selected results of tests performed on soda-lime-silica glass and alumina are presented to show the effectiveness of the technique. Normal glass microscope slides or alumina plates were used as test specimens. These were cut to have the approximate dimensions shown in Fig. 3. A crack was initiated in the groove by tightening a sharpened screw against the ungrooved side. The specimen was then inserted into the loading arms and the load applied. Values of T up to 800 g were required for the glass specimens, while loads of up to 2000 g were used for the alumina. Crack lengths were measured for the most part with a travelling microscope having an accuracy of $\pm$ 0.0005 mm, although some use was made of the compliance technique. A number of different constant $\mathcal{G}$ tests were obtained on the same specimen by stepping the load appropriately.

All measurements of specimen geometry were made after the crack had progressed completely through the sample. Determinations of W, h, and t, were made at a number of points in the crack path using the travelling microscope. It was necessary to take into account the presence of the groove in order to obtain an accurate value of moment of inertia. An average value of I for each side of the specimen was used in the calculation of $\mathcal{G}$.

Typical plots of crack length versus time are shown in Fig. 5. The slope of these curves is the crack velocity at each $\mathcal{G}$. It can be seen that this velocity is independent of crack length as would be expected for glass under these loading conditions. Crack velocities determined by the compliance technique agreed within $\pm$ 10% of those obtained visually.

Fig. 6 shows a plot of K versus log velocity for soda-lime-silica glass in three different environments, where K is the stress intensity factor for

*Moog Inc.
†Direct current differential transformer.

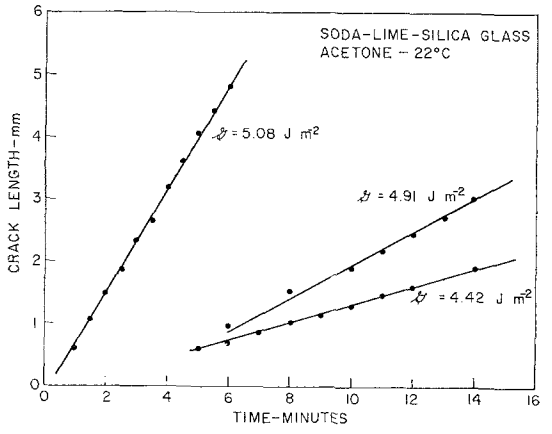

Figure 5 Crack length as a function of time in soda-lime-silica glass at various levels of strain energy release rate.

plane stress, $K = \sqrt{(\mathscr{G}E)}$. Because of the small changes in $\mathscr{G}$ or K in relation to the changes in velocity, both semi-log and log-log plots give similar curves. As can be seen from the data taken in octanol, the relationship between K and velocity need not be simple, but depends on the test material and environment. As shown, similar results are obtained using a conventional double cantilever arrangement [8] or through the use of a double-torsion specimen loaded in a constant deflection mode [6].

The data for Al_2O_3 shown in Fig. 7 was more scattered possibly because of the greater inhomogeneity of polycrystalline material compared to glass. In many instances cracks were observed to decelerate or accelerate at a constant $\mathscr{G}$, suggesting that dV/dt terms may be important in the analysis of crack growth.

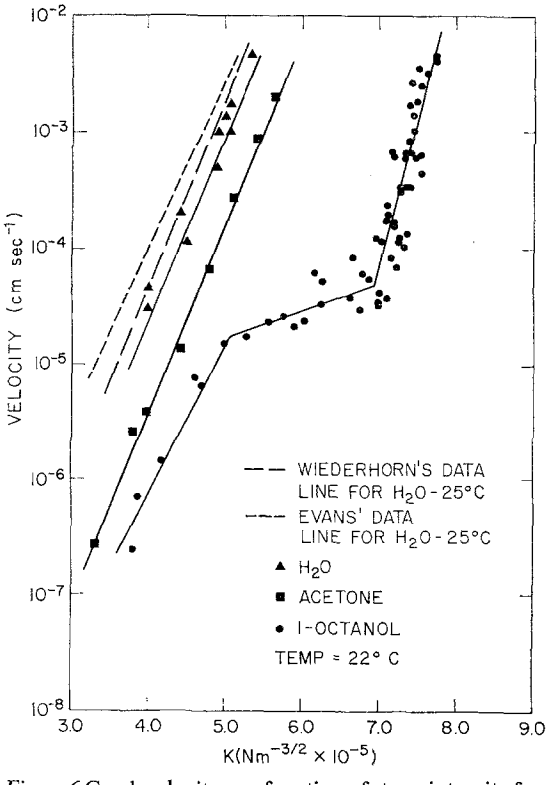

Figure 6 Crack velocity as a function of stress intensity factor for soda-lime-silica glass in different liquid environments. Comparison of data taken in distilled H_2O is made with that reported by Evans [6] and Wiederhorn [8] using different techniques.

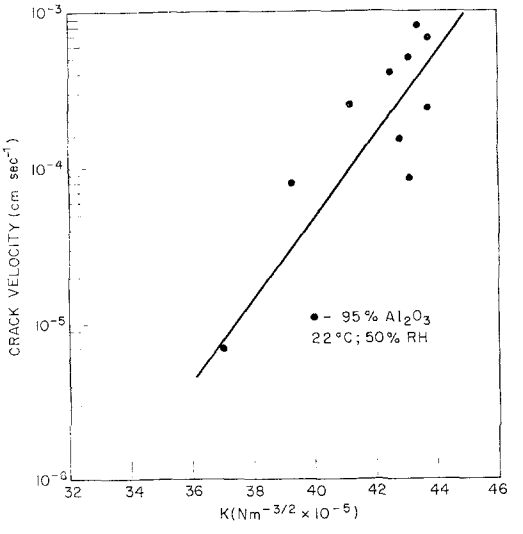

Figure 7 K-velocity relationship for a commercial alumina in air at 22°C, 50% r.h.

5. Summary

A general analysis of crack growth in double cantilever beams using beam and beam on elastic foundation theory was presented, in which contributions to strain energy release rate owing to plastic deformation, shear, and other deformations are considered. It was observed from the expressions for $\mathscr{G}$ obtained in this analysis, that a simple test results if a constant bending moment is applied to the beam. In this configuration, $\mathscr{G}$ is independent of crack length and plastic zone size (provided $dr = 0$) and contributions to $\mathscr{G}$ owing to shear or rotations ahead of the crack are zero.

Results of investigations on soda-lime-silica glass and Al_2O_3 showed the above technique to be effective in obtaining the relationship between $\mathscr{G}$ (or K) and crack velocity. It was also shown that crack velocities could be accurately

determined by either a visual observation or measurement of compliance changes in the loading system.

Appendix

Analysis of double cantilever beam specimens

This analysis is based on the specimen configuration shown in Figs. A1 and A2. For analysis

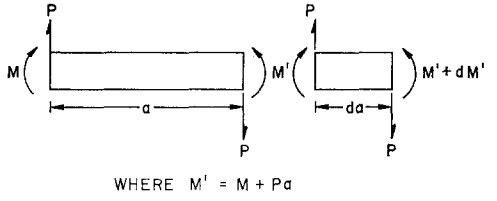

Figure A1 Detailed schematic drawing of cantilever beam portion of specimen.

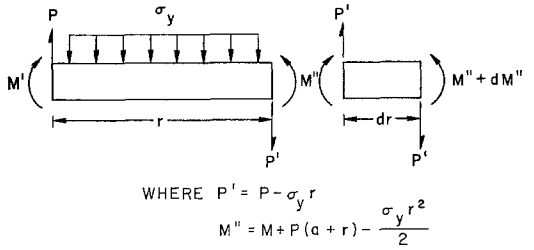

Figure A2 Detailed schematic drawing of plastic zone portion of specimen.

purposes, the specimen is divided into three parts.

1. Cantilever Beam

Bending.

$$dw = \frac{da}{2EI}(M')^2 \tag{A1}$$

$$= \frac{da}{2EI}(M + Pa)^2 \tag{A2}$$

Shear.

$$dw = \frac{P^2}{2GA}\,da \tag{A3}$$

The total change in stored elastic energy is

$$\frac{dw}{da} = \frac{1}{2EI}\left[(M + Pa)^2 + \frac{EIP^2}{GA}\right]. \tag{A4}$$

2. Plastic zone

Bending.

$$dw = \frac{dr}{2EI}\left[M + P(a + r) - \frac{\sigma_y r^2}{2}\right] \tag{A5}$$

Shear.

$$dw = \frac{dr}{2GA}(P - \sigma_y r)^2 \tag{A6}$$

so

$$\frac{dw}{dr} = \frac{1}{2EI}\left\{\left[M + P(a + r) - \frac{\sigma_y r^2}{2}\right]^2 + \frac{EI}{GA}(P - \sigma_y r)^2\right\} \tag{A7}$$

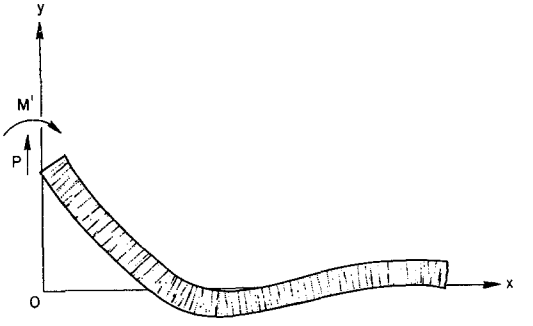

Figure A3 Deflection of beam on elastic foundation (after Hetenyi [9]).

3. Beam on elastic foundation (see Figs. 2 and A3)

$$\text{web modulus} = k = \frac{tE}{w}$$

From beam on elastic foundation theory [9]

$$\frac{d^4u}{dx^4} + \frac{k}{EI}u = 0. \tag{A8}$$

The characteristic roots for this equation are

$$\lambda^4 = \frac{1}{\delta^4} = \frac{k}{4EI} \tag{A9}$$

where δ is the characteristic length of the beam.

The total energy is given by one half the product of the loads and moments times the displacements and rotations of the beam

$$W = 1/2\left\{P'M''\right\}\left\{\begin{matrix}u\\ \theta\end{matrix}\right\} \tag{A10}$$

where P' and M'' are defined in Fig. A2.

From Hetenyi [9] the deflections and rotations of a semi-infinite beam on an elastic foundation can be given in matrix form as

$$\left\{\begin{matrix}u\\ \theta\end{matrix}\right\} = \frac{\delta}{2EI}\begin{bmatrix}\delta^2 & \delta\\ \delta & 2\end{bmatrix}\left\{\begin{matrix}P'\\ M''\end{matrix}\right\}. \tag{A11}$$

Substituting for $\begin{Bmatrix} u \\ \theta \end{Bmatrix}$ in A10

$$W = \frac{\delta}{4EI} \begin{Bmatrix} P' M'' \end{Bmatrix} \begin{bmatrix} \delta^2 & \delta \\ \delta & 2 \end{bmatrix} \begin{Bmatrix} P' \\ M'' \end{Bmatrix} \cdot \quad \text{(A12)}$$

Performing the matrix multiplication

$$W = \frac{\delta}{2EI} \left[\frac{\delta^2 P'^2}{2} + \delta M'' P' + M''^2 \right] \quad \text{(A13)}$$

and

$$\mathrm{d}W = \frac{\partial W}{\partial a} \mathrm{d}a + \frac{\partial W}{\partial r} \mathrm{d}r \cdot \quad \text{(A14)}$$

Under most test conditions, some of the parameters in Equation A13 will vanish so that a relatively simple expression for W will be obtained.

The total change in elastic energy with an increase in crack and/or plastic zone size is given by a combination of Equations A4, A6, A13 and A14.

Linear viscoelastic materials can also be analysed, by using expressions derived by Wnuk [10]. The viscoelastic displacement in the vicinity of the tip of a slowly moving crack is the product of the elastic displacement and the compliance function $\psi(\triangle/V)$. Using this result in the analysis of the cantilever beam specimen, the displacement owing to bending becomes

$$\mathrm{d}u_{\text{viscoelastic}} = \mathrm{d}u_{\text{elastic}} \, \psi(\triangle/V) \quad \text{(A15)}$$
$$= \frac{M' a \mathrm{d}a}{EI} \psi(\triangle/V)$$

and the change in stored energy is

$$\mathrm{d}W = \frac{1}{2} M' \mathrm{d}\theta = \frac{M'^2 \mathrm{d}a}{2EI} \psi(\triangle/V) \cdot \quad \text{(A16)}$$

Similarly, the displacement owing to shear becomes

$$\mathrm{d}u_{\text{viscoelastic}} = \mathrm{d}u_{\text{elastic}} \, \psi(\triangle/V) \quad \text{(A17)}$$
$$= \frac{P \mathrm{d}a}{AG} \psi(\triangle/V)$$

and the change in stored energy is

$$\mathrm{d}W = \frac{1}{2} P \mathrm{d}a = \frac{P^2 \mathrm{d}a}{2AG} \psi(\triangle/V) \cdot \quad \text{(A18)}$$

Consequently, in Equation A19, the $\mathcal{G}_{\text{viscoelastic}}$ is obtained from $\mathcal{G}_{\text{elastic}}$ by forming the product with the compliance function $\psi(\triangle/V)$. Applying this analysis to the double cantilever specimen, the strain energy release rate to propagate a crack becomes

$$\mathcal{G}_{\text{vE}} = \mathcal{G} \, \psi(\triangle/V) \quad \text{(A19)}$$

where for the standard linear model,

$$\psi(\triangle/V) = 1 + \frac{E_1}{E_2} \left[1 - \exp\left(\frac{-\triangle}{V} \right) \right] \quad \text{(A20)}$$

and $\mathcal{G}$ was obtained using the previously discussed techniques.

Acknowledgements

The authors would like to thank Mr G. P. Kendrick for preparing the specimens and Mr P. C. Miller for his help in obtaining the data.

References

1. E. J. RIPLING, S. MOSTOVOY and R. L. PATRICK, *Mat. Res. and Stand.* **4** (1964) 129.
2. P. P. GILLIS and J. J. GILMAN, *J. Appl. Phys.* **35** (1961) 647.
3. S. M. WIEDERHORN, A. M. SHORB, and R. L. MOSES. *ibid* **39** (1968) 1569.
4. J. O. OUTWATER and M. C. MURPHY, Final Report Contract No. DAAA 21-67-C-0041 (1970).
5. J. A. KIES and A. B. J. CLARK, Proceedings of the Second International Conference on Fracture; Brighton, England, Paper 41 (1969).
6. A. G. EVANS, *J. Mater. Sci.* **7** (1972) 1137.
7. E. J. RIPLING, S. MOSTOVOY, and P. B. CROSELY. *J. Mats.* **2** (1967) 661.
8. S. M. WIEDERHORN, *J. Amer. Ceram. Soc.* **50** (1967) 407.
9. M. HETENYI "Beams on Elastic Foundation" (University of Michigan Press, Ann Arbor, Michigan, 1946) p. 24.
10. M. P. WNUK, Final Report, Contract N00014-70-C-0077 (1970).

Received 27 February and accepted 21 May 1973.